arXiv:1404.4804v2 [q-bio.PE] 13 Oct 2014

Dynamical transitions in a pollination–herbivory interaction: a conflict between mutualism and antagonism

Tomás A. Revilla[1] and Francisco Encinas-Viso[2]

[1]Centre for Biodiversity Theory and Modelling, 09200 Moulis, France.
Email:tomrevilla@gmail.com
[2]CSIRO Plant Industry, GPO Box 1600, Canberra, ACT 2601, Australia.
Email:francisco.encinas.viso@csiro.au

October 14, 2014

Abstract

Plant-pollinator associations are often seen as purely mutualistic, while in reality they can be more complex. Indeed they may also display a diverse array of antagonistic interactions, such as competition and victim–exploiter interactions. In some cases mutualistic and antagonistic interactions are carried-out by the same species but at different life-stages. As a consequence, population structure affects the balance of inter-specific associations, a topic that is receiving increased attention. In this paper, we developed a model that captures the basic features of the interaction between a flowering plant and an insect with a larval stage that feeds on the plant's vegetative tissues (e.g. leaves) and an adult pollinator stage. Our model is able to display a rich set of dynamics, the most remarkable of which involves victim–exploiter oscillations that allow plants to attain abundances above their carrying capacities, and the periodic alternation between states dominated by mutualism or antagonism. Our study indicates that changes in the insect's life cycle can modify the balance between mutualism and antagonism, causing important qualitative changes in the interaction dynamics. These changes in the life cycle could be caused by a variety of external drivers, such as temperature, plant nutrients, pesticides and changes in the diet of adult pollinators.

Keywords: *mutualism, pollination, herbivory, insects, stage-structure, oscillations*

1 Introduction

Il faut bien que je supporte deux ou trois chenilles si je veux connaître les papillons

Le Petit Prince, Chapitre IX – Antoine de Saint-Exupéry

Mutualism entails costs in addition to benefits. Conflicting goals can lead to cheating where one party incurs the cost of providing energy to enable mutualism, while the other exploits, but does not reciprocate (e.g. nectar robbers). There can also be costs concerning other detrimental interactions that run in parallel with mutualism, such as predation, parasitism or competition involving the same parties. Moreover, some of these antagonistic interactions (e.g. competition) seem to be important for the evolution and stability of mutualism (Jones et al., 2012). In general, these costs have important consequences at the population and community level, because the net outcome can turn out beneficial or detrimental, but perhaps more interestingly, variable (Bronstein, 1994). Variable interactions challenge the view that ecological communities are structured by well defined interactions at the species level such as competition (–,–), victim-exploiter (–,+) or mutualism (+,+).

Pollination is one of the most important mutualisms occurring between plants and animals. This form of trading resources for services greatly explains the evolutionary success of flowering plants in almost all terrestrial systems. It is responsible for the well being of ecosystem services. During the larval stage of many insect pollinators, such as Lepidopterans (butterflies and moths), the larvae feed on plant leaves to mature and become adult pollinators (Adler and Bronstein, 2004; Wäckers et al., 2007; Bronstein et al., 2009; Altermatt and Pearse, 2011). These ontogenetic diet shifts (Rudolf and Lafferty, 2011) are very common and important in understanding the ecological and evolutionary dynamics of plant–animal mutualisms. Interestingly, in some cases larvae feed on the same plant

species that they will pollinate as adults (Irwin, 2010; Bronstein et al., 2009). This shows that in several cases mutualistic and antagonistic interactions are exerted by the same species. and a potential conflict arises for the plant. between the benefits of mutualism and the costs of herbivory. One of the best known examples is the interaction between tobacco plants (*Nicotiana attenuata*) and the hawkmoth (*Manduca sexta*) (Baldwin, 1988; Kessler et al., 2010), whose larva is commonly called the tobacco hornworm. There are other examples of this type of interaction in the genus *Manduca* (Sphingidae), such as between the tomato plant (*Lycopersicon esculentum*) and the five-spotted hawkmoth (*Manduca quinquemaculata*) (Kennedy, 2003). These larvae have received a lot of attention due to their negative effects on agricultural crops (Campbell et al., 1991).

The interaction between *Manduca sexta* and *Datura wrightii* (Solanacea) (Bronstein et al., 2009; Alarcon et al., 2008) is another good example illustrating the costs and benefits of pollination mutualisms (Bronstein et al., 2009). *D. wrightii* provides high volumes of nectar and seems to depend heavily on the pollination service by *M. sexta* adults (Alarcon et al., 2008). However, *M. sexta* larvae, which feed on *D. wrightii* vegetative tissue, can have severe negative effects on plant fitness (McFadden, 1968; Barron-Gafford et al., 2012). We could assume that the benefits of pollination might outweigh the costs of herbivory for this mutualism to be relatively viable. The question is what are the conditions, in terms of benefits (pollination) and costs (herbivory), for this mutualistic interaction to be stable?

In the pollination–herbivory cases mentioned previously the benefits and costs for the plant are clearly differentiated. This is because the role of an insect as a pollinator or herbivore depends on the stage in its life cycle (Miller and Rudolf, 2011). Thus, whether mutualism or herbivory dominates the interaction is dependent on insect abundance and its population structure. In other words the *cost:benefit* ratio must be positively related with the insect's *larva:adult* ratio. For a hypothetical scenario in which the costs of herbivory (–) and the benefits of pollination (+) are balanced for the plant (0), an increase in larval abundance relative to adults should bias the relationship towards a victim-exploiter one (–,+). Whereas an increase in adult abundance relative to larvae should bias the relationship towards mutualism (+,+). Under equilibrium conditions, one would expect transitions (bifurcations) from (–,+) to (0,+) to (+,+) and vice-versa as relevant parameters affecting the plant and the insect life-histories vary, such as flower production, mortalities or larvae maturation rates. However, under dynamic scenarios the outcome may be more complex: a victim–exploiter state (–,+) enhances larva development into pollinating adults, but this tips the interaction into a mutualism (+,+), which in turn contributes greater production of larva leading back to a victim–exploiter state (–,+). This raises the possibility of feedback between the plant–insect interaction and insect population structure, which can potentially lead to periodic alternation between mutualism and herbivory. Thus, when non-equilibrium dynamics are involved, questions concerning the overall nature (positive, neutral or negative) of mixed interactions may not have simple answers.

In this article we study the feedback between insect population structure, pollination and herbivory. We want to understand how the balance between costs (herbivory) and benefits (pollination) affects the interaction between plants (e.g. *D. wrightii*) and herbivore–pollinator insects (e.g. *M. sexta*)? Also what role does insect development have in this balance and on the resulting dynamics? We use a mathematical model which considers two different resources provided by the same plant species, nectar and vegetative tissues. Nectar consumption benefits the plant in the form of fertilized ovules, and consumption of vegetative tissues by larvae causes a cost. Our model predicts that the balance between mutualism and antagonism, and the long term stability of the plant–insect association, can be greatly affected by changes in larval development rates, as well as by changes in the diet of adult pollinators.

2 PLA (plant-larva-adult) model

Our model concerns the dynamics of the interaction between a plant and an insect. The insect life cycle comprises an adult phase that pollinates the flowers and a larval phase that feed on non-reproductive tissues of the same plant. Adults oviposit on the same species that they pollinate (e.g. *D. wrightii* – *M. sexta* interaction). Let denote the biomass densities of the plant, the larva, and the adult insect with P, L and A respectively. An additional variable, the total biomass of flowers F, enables the mutualism by providing resources to the insect (nectar), and by collecting services for the plant (pollination). The relationship is *facultative–obligatory*. In the absence of the insect, the plant's vegetative biomass grows logistically, preventing its extinction. In the absence of the plant however, the insect always goes extinct because larval development relies exclusively on herbivory, even if the adults pollinate other plant species. This is based on the biology of *M. sexta* (Bronstein et al., 2009). The mechanism of interaction between these four variables (P, L, A, F) is described by the following system of ordinary differential equations (ODE):

$$\begin{aligned}
\frac{dP}{dt} &= rP(1-cP) + \sigma aFA - bPL \\
\frac{dF}{dt} &= sP - wF - aFA \\
\frac{dL}{dt} &= \epsilon aFA + gA - \gamma bPL - mL \\
\frac{dA}{dt} &= \gamma bPL - nA
\end{aligned} \tag{1}$$

where r: plant intrinsic growth rate, c: plant intra-specific self-regulation coefficient (also the inverse its carrying capacity), a: pollination rate, b: herbivory rate, s : flower production rate, w: flower decay rate, m, n: larva and adult mortality rates, σ: plant pollination efficiency ratio, ϵ: adult consumption efficiency ratio. Like ϵ, parameter γ is also a consumption efficiency ratio, but we will call it the maturation rate for brevity since we will refer to it frequently. Our model assumes that pollination leads to flower closure (Primack, 1985), causing resource limitation for adult insects. Parameter g represents a reproduction rate resulting from the pollination of other plants species, which we do not model explicitly. Most of our results are for $g = 0$.

We now consider the fact that flowers are ephemeral compared with the life cycles of plants and insects. In other words, some variables (P, L, A) have slower dynamics, and others (F) are fast (Rinaldi and Scheffer, 2000). Given the near constancy of plants and animals in the flower equation of (1), we can predict that flowers will approach a quasi-steady-state (or quasi-equilibrium) biomass $F \approx sP/(w + aA)$, before P, L and A can vary appreciably. Substituting the quasi-steady-state biomass in system (1) we arrive at:

$$\begin{aligned}
\frac{dP}{dt} &= rP(1-cP) + \sigma \left[\frac{asA}{w+aA}\right] P - bPL \\
\frac{dL}{dt} &= \epsilon \left[\frac{asP}{w+aA}\right] A + gA - \gamma bPL - mL \\
\frac{dA}{dt} &= \gamma bPL - nA
\end{aligned} \tag{2}$$

In system (2) the quantities in square brackets can be regarded as functional responses. Plant benefits saturate with adult pollinator biomass, i.e. pollination exhibits diminishing returns. The functional response for the insects is linear in the plant biomass, but is affected by intraspecific competition (Schoener, 1978) for mutualistic resources.

We non-dimensionalized this model to reduce the parameter space from 12 to 9 parameters, by casting biomasses with respect to the plant's carrying capacity $(1/c)$ and time in units of plant biomass renewal time $(1/r)$. This results in a PLA (plant, larva, adult) scaled model:

$$\begin{aligned}
\frac{dx}{d\tau} &= x(1-x) + \sigma \frac{\alpha z}{\eta + z} x - \beta xy \\
\frac{dy}{d\tau} &= \epsilon \frac{\alpha x}{\eta + z} z + \phi z - \gamma \beta xy - \mu y \\
\frac{dz}{d\tau} &= \gamma \beta xy - \nu z
\end{aligned} \tag{3}$$

Table 1 lists the relevant transformations.

There is an important clarification to make concerning the nature and scales of the conversion efficiency ratios σ, ϵ involved in pollination, and γ for herbivory and maturation. This has to do with the fact that flowers *per se* are not resources or services, but *organs* that enable the mutualism to take place, and they mean different things in terms of biomass production for plants and animals. For insects, the yield of pollination is thermodynamically constrained. First of all, a given biomass F of flowers contains an amount of nectar that is necessarily less than F. More importantly, part of this nectar is devoted to survival, or wasted, leaving even less for reproduction. Similarly, not all the biomass consumed by larvae will contribute to their maturation to adult. *Ergo* $\epsilon < 1, \gamma < 1$. Regarding the returns from pollination for the plants, the situation is very different. Each flower harbors a large number of ovules, thus a potentially large number of seeds (Fagan et al., 2014), each of which will increase in biomass by consuming resources not considered by our model (e.g. nutrients, light). Consequently, a given biomass of pollinated flowers can produce a larger biomass of mature plants, making σ larger than 1.

Table 1: Variables and parameters of the scaled PLA model (3) and values used for numerical analyses. The last column shows a corresponding set of parameter values in the unscaled version of the same model (2), for plant carrying capacities of $c^{-1} = 100$ biomass units, and $r^{-1} = 20$ time units.

Symbol	Description	Value	$c = 0.01, r = 0.05$
$x = cP, y = cL, z = cA$	plant, larval and adult biomass	variable	
$\tau = rt$	time	variable	
$\alpha = s/r$	asymptotic pollination rate	5	$s = 0.25$
$\eta = wc/a$	half-saturation constant of pollination	0.1	$w = 0.5$ & $a = 0.05$
$\beta = b/rc$	herbivory rate	0 to 100	$b = 0$ to 0.05
$\mu = m/r$	larva mortality rate	1	$m = 0.05$
$\nu = n/r$	adult mortality rate	2	$n = 0.1$
$\phi = g/r$	insect intrinsic reproduction rate	0 or 1	$g = 0$ or 0.05
σ	plant pollination conversion ratio	5	
ϵ	insect pollination conversion ratio	0.5	
γ	maturation rate (herbivory conversion ratio)	0 to 0.1	

3 Results

The PLA model (3) has many parameters, however here we focus on herbivory rates (β) and larvae maturation (γ), because increasing β turns the net balance interaction towards antagonism, whereas increasing γ shifts insect population structure towards the adult phase, turning the net balance towards mutualism. Both parameters also relate to the state variables at equilibrium (i.e. $z/y = \beta\gamma x/\nu$ in (3 for $dz/d\tau = 0$). In section 3.1 we studied the joint effects of varying β and γ numerically (parameter values in Table 1). In section 3.2 we present a simplified graphical analysis of our model, in order to explain how different dynamics can arise, by varying β, γ and other parameters.

3.1 Numerical results

Figure 1 shows interaction outcomes of the PLA model, as a function of β and γ for specialist pollinators ($\phi = 0$). This parameter space is divided by a decreasing $R_o = 1$ line that indicates whether or not insects can invade when rare. R_o is defined as (see derivation in Appendix A):

$$R_o = \frac{\epsilon\alpha\gamma\beta}{\eta\nu(\mu + \gamma\beta)} \tag{4}$$

and we call it the *basic reproductive number*, according to the argument that follows. Consider the following in system (3): if the plant is at carrying capacity ($x = 1$), and is invaded by a very small number of adult insects ($z \approx 0$), the average number of larvae produced by a single adult in a given instant is $\epsilon\alpha x/(\eta+z) \approx \epsilon\alpha/\eta$, and during its life-time (ν^{-1}) it is $\epsilon\alpha/\eta\nu$. Larvae die at the rate μ, or mature with a rate equal to $\gamma\beta x = \gamma\beta$, per larva. Thus, the probability of larvae becoming adults rather than dying is $\gamma\beta/(\mu + \gamma\beta)$. Multiplying the life-time contribution of an adult by this probability gives the expected number of new adults replacing one adult per generation during an invasion (R_o). More formally, R_o is the expected number of adult-insect-grams replacing one adult-insect-gram per generation (assuming a constant mass-per-individual ratio).

Below the $R_o = 1$ line, small insect populations cannot replace themselves ($R_o < 1$) and two outcomes are possible. If the maturation rate is too low, the plant only equilibrium ($x = 1, y = z = 0$) is globally stable and plant–insect coexistence is impossible for all initial conditions. If the maturation rate is large enough, stable coexistence is possible, but only if the initial plant and insect biomass are large enough. This is expected in models where at least one species, here the insect, is an obligate mutualist. In this region of the space of parameters, the growth of small insect populations increases with population size, a phenomenon called the Allee effect (Stephens et al., 1999).

Above the $R_o = 1$ line the plant only equilibrium is always unstable against the invasion of small insect populations ($R_o > 1$). Plants and insects can coexist in a stable equilibrium or via limit cycles (stable oscillations). The zone of limit cycles occurs for intermediate values of the maturation rate (γ) and it widens with rate of herbivory (β).

Plant equilibrium when coexisting with insects can be above or below the carrying capacity ($x = 1$). When above carrying capacity the net result of the interaction is a mutualism (+,+). While in the second case we have

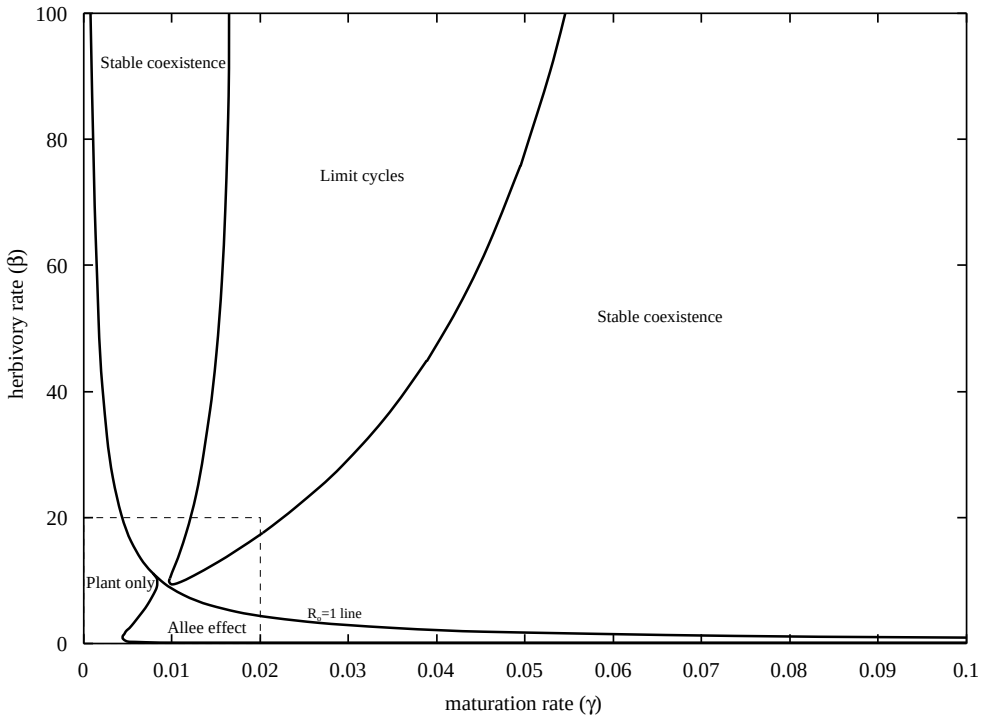

Figure 1: Outcomes of the PLA model as a function of the larval maturation and herbivory rates for specialist pollinators ($\phi = 0$). The rectangular region in the bottom left is analyzed with more detail in Appendix A.

antagonism, more specifically net herbivory (−,+). As it would be expected, increasing herbivory rates (β) shifts this net balance towards antagonism (low plant biomass), while decreasing it shifts the balance towards mutualism (high plant biomass). The quantitative response to increases in the maturation rate (γ) is more complex however (see the bifurcation plot in Appendix A).

Given that there is herbivory, we encounter victim–exploiter oscillations. However, the oscillations in the PLA model are special in the sense that the plant can attain maximum biomasses above the carrying capacity ($x > 1$). For an example see Figure 2. Instead of a stable balance between antagonism and mutualism, we can say that the outcome in Figure 2 is a periodic alternation of both cases. This is not seen in simple victim–exploiter models, where oscillations are always below the victim's carrying capacity (Rosenzweig and MacArthur, 1963; Rosenzweig, 1971). The relative position of the cycles along the plant axis is also affected by herbivory: if β decreases (increases), plant maxima and minima will increase (decrease) in Figure 2 (see bifurcation plot in Appendix A). In some cases the entire plant cycle (maxima and minima) ends above the carrying capacity if β is low enough (see Appendix C), but further decrease causes damped oscillations. We also found examples in which coexistence can be stable or lead to limit cycles depending on the initial conditions (see example in Appendix C), but this happens in a very restrictive region in the space of parameters (see bifurcation plot in Appendix A). Limit cycles can also cross the plant's carrying capacity under the original interaction mechanism (1), which does not assume the steady–state in the flowers (see an example in Appendix C, which uses the parameter of the last column in Table 1).

Figure 3 shows the β vs γ parameter space of the model when the adults are more generalist. The relative positions of the plant-only, Allee effect, and coexistence regions are similar to the case of specialist pollinators (Figure 1). However, the region of limit cycles is much larger. The $R_0 = 1$ line is closer to the origin, because the expression for R_0 is now (see derivation in Appendix A):

$$R_0 = \frac{(\epsilon\alpha + \phi\eta)\gamma\beta}{\eta\nu(\mu + \gamma\beta)} \tag{5}$$

In other words, this means that the more generalist the adult pollinators (larger ϕ), the more likely they can invade when rare. There is also a small overlap between the Allee effect and limit cycle regions, i.e. parameter combinations for which the long term outcome could be insect extinction or plant–insect oscillations, depending on the initial conditions.

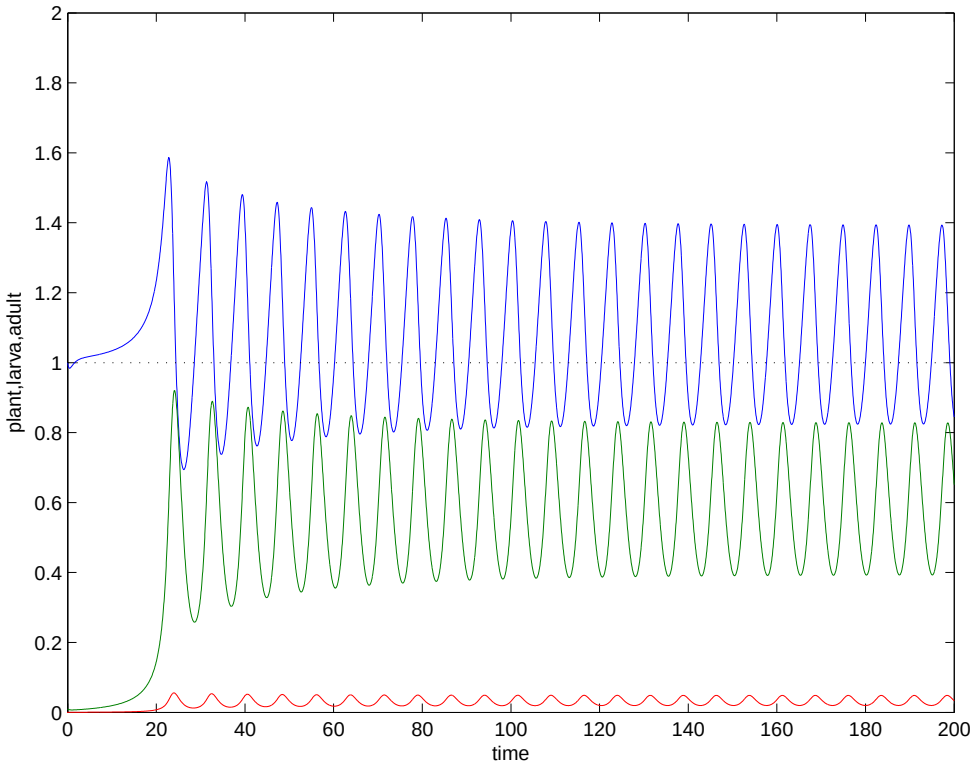

Figure 2: Limit cycles in the PLA model (3) with plant biomasses alternating above and below the carrying capacity (dotted line). Parameters as in Table 1, with $\gamma = 0.01, \beta = 10$. Blue:plant, green:larva, red:adult.

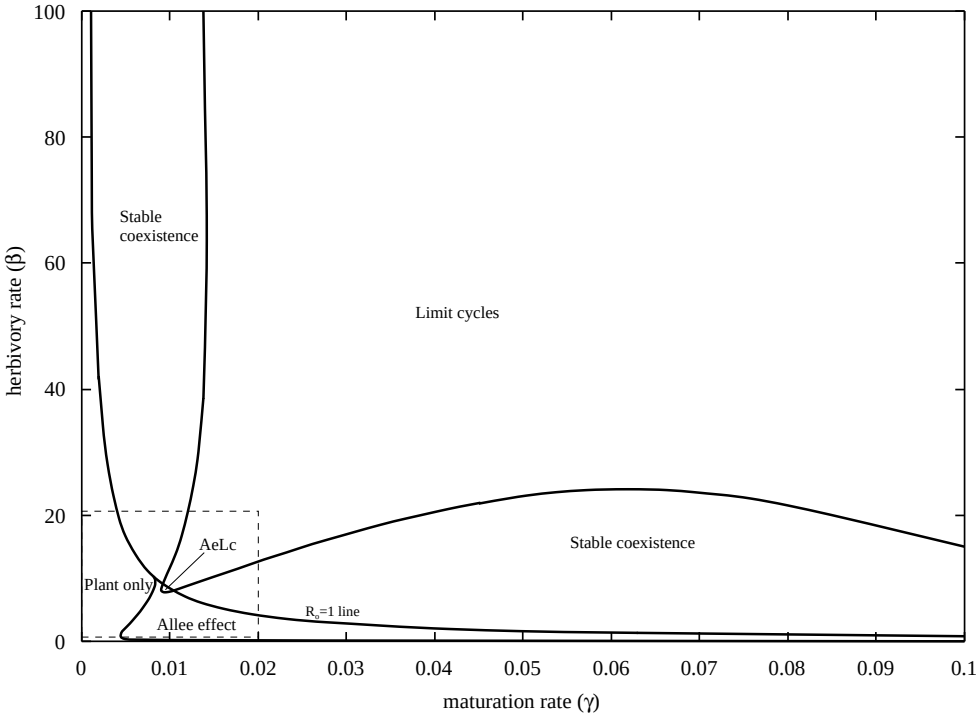

Figure 3: Outcomes of the PLA model as a function of the larval maturation and herbivory rates for generalist pollinators ($\phi = 1$). AeLc: intersection of the Allee effect and Limit cycle zones.

3.2 Graphical analysis

The general features of the interaction can be studied by phase-plane analysis. To make this easier, we collapsed the three-dimensional PLA model into a two-dimensional plant–larva (PL) model, by assuming that adults are extremely short lived compared with plants and larvae (see resulting ODE in Appendix B). The closest realization of this assumption could be *Manduca sexta*, which has a larval stage of approximately 20-25 days and adult stages of around 7 days (Reinecke et al., 1980; Ziegler, 1991). For a given parametrization (Table 1), the PL model has the same equilibria as the PLA model, but not the exact same global dynamics due to the alteration of time scales. Yet, this simplification provides insights about the outcomes displayed in Figures 1 and 3.

Figure 4 shows plant and larva isoclines (i.e. non-trivial nullclines) and coexistence equilibria (intersections). Isocline properties are analytically justified (Appendix B). These sketches are grossly exaggerated, but this facilitates the representation of features that are hard to notice by plotting them numerically (e.g. with parameters like in Table 1).

Plant isoclines take two main forms:

$$\begin{cases} \gamma\sigma\alpha < \eta\nu & \text{the isocline lies entirely below (to the left of) the carrying capacity} \\ \gamma\sigma\alpha > \eta\nu & \text{parts of the isocline lie above (to the right of) the carrying capacity} \end{cases} \tag{6}$$

In both cases, plants grow between the isocline and the axes, and decrease otherwise. Larva isoclines are simpler, they start in the plant axis and bend towards the right when insects tend towards specialization ($\phi < \nu$). When insects tend towards generalism ($\phi > \nu$), their isoclines increase rapidly upwards like the letter "J" (not shown here, see Appendix B) . Insects grow below and right of the larva isocline, and decrease otherwise.

The $\gamma\sigma\alpha < \eta\nu$ case in Figure 4A covers scenarios in which pollination rates (α), plant benefits (σ), adult pollinator lifetimes ($1/\nu$) and larva-to-adult transition rates (γ) are low. The plant's isocline is a decreasing curve crossing the plant's axis at its carrying capacity K ($x = 1, y = 0$). Coexistence is unfavorable for the plant since its equilibrium biomass lies below the carrying capacity ($x < 1$). The local dynamics around the coexistence equilibrium indicates oscillations, and we can use the geometry of the intersection to infer that the equilibrium is stable (eigenvalue analysis is too difficult to perform for this model): Figure 4A shows that if plants increase (or decrease) above the equilibrium while keeping the insect density fixed, they enter a zone of negative (or positive) growth; and the same holds for the insects while keeping the plants fixed. In ecological terms, both species are self-limited around the coexistence equilibrium, which as a rule of thumb is a strong indication of stability (Case, 2000). Together with the fact that the trivial ($x = 0, y = 0$) and carrying capacity equilibrium ($x = 1, y = 0$) are saddle points, we conclude that plants and insects achieve an equilibrium after a period of transient oscillations (provided that insects are viable, e.g. β, γ, ϵ are large enough). Indeed, for extreme scenarios of negligible plant pollination benefits (i.e. α and/or σ tend to zero), the plant's isocline approximates a straight line with a negative slope, like the isocline of a logistic prey in a Lotka–Volterra model, which is well known to cause damped oscillations (Case, 2000).

The $\gamma\sigma\alpha > \eta\nu$ case in Figures 4B,C,D covers scenarios in which pollination rates (α), pollination benefits (σ), adult pollinator lifetimes ($1/\nu$) and larva-to-adult (harm-to-benefit) transition rates (γ) are high. One part of the plant's isocline lies above the carrying capacity, which means that coexistence equilibria with plant biomass larger than the carrying capacity ($x > 1$) are possible; this is favorable for the plant. The isocline also displays a "hump" like in the classical victim–exploiter models (Rosenzweig and MacArthur, 1963). Intersections at the right of the hump would lead to damped oscillations, like in Figure 4A (for $\gamma\sigma\alpha < \eta\nu$). Intersections at the left of the hump, like in Figure 4B, suggest oscillations that will increase in amplitude. This is because a small increase (decrease) along the plant's axis leaves the plant at the growing (decreasing) side of its isocline, promoting further increase. This means that plants do not experience self-limitation, a rule-of-thumb indicator of instability (Case, 2000) and we infer that interactions would not dampen, leading to limit cycles. We have seen in Figure 2 that limit cycles can pass above the plant's carrying capacity, which is implied in Figure 4B, by picturing the maximum of the plant's hump at the right of carrying capacity, and the intersection of isoclines between both points. Even if the hump lies at left of the carrying capacity, we cannot use this graphical analysis to discard the possibility of limit cycles overcoming the carrying capacity.

For $\gamma\sigma\alpha > \eta\nu$ the plant's isocline also "folds" from its rightmost extent back towards the carrying capacity point. An intersection with this fold is shown in Figure 4C, resulting in an equilibrium above the plant's carrying capacity ($x > 1$), which is approached without oscillations. Intersections can also result in two equilibria, in which one of them is always unstable and belongs to a threshold above which insect invasion is possible (and not possible if below) (Figure 4D). This explains the Allee effect, i.e. insect intrinsic growth rates increase from negative to positive as insect initial density increases.

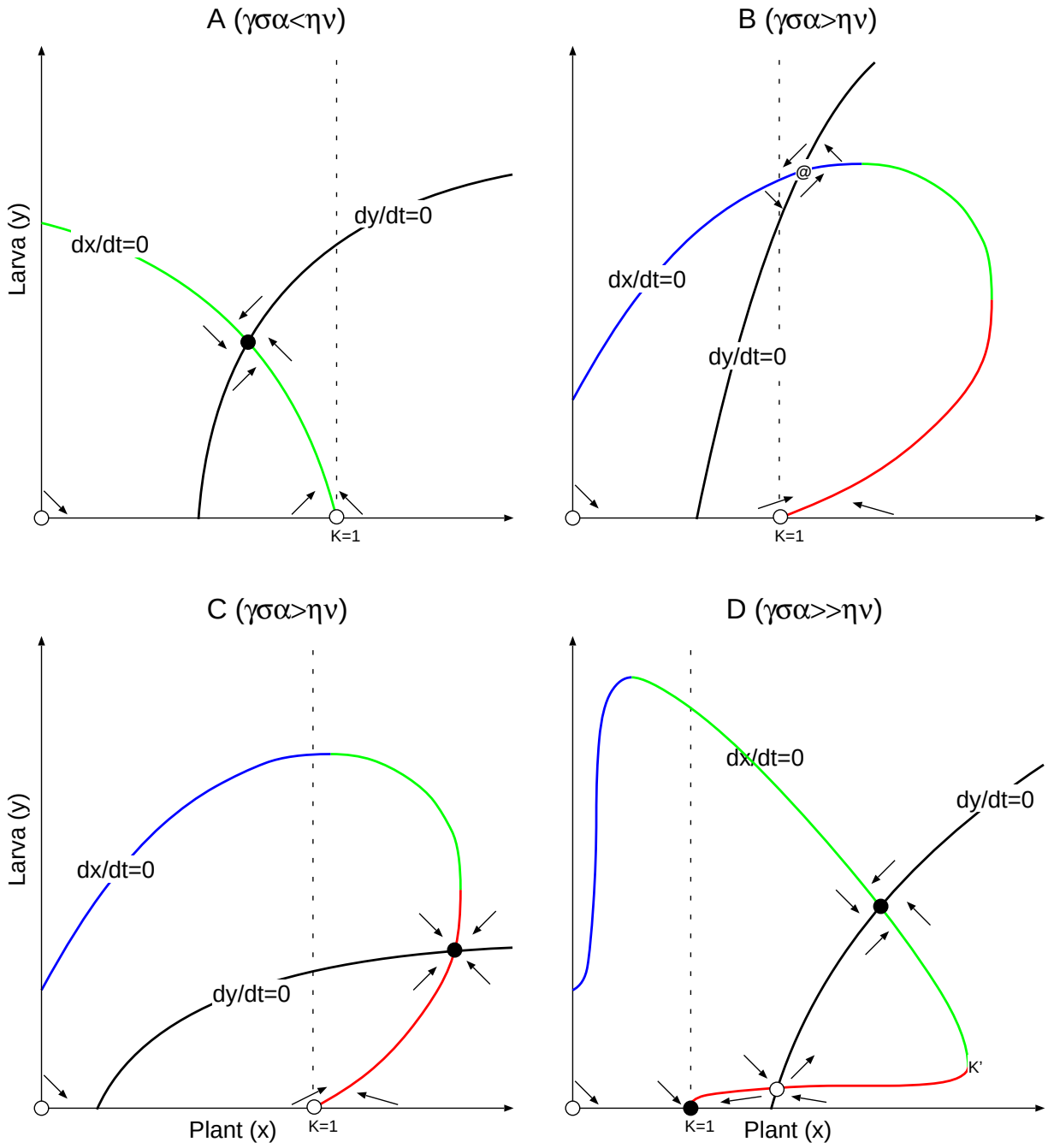

Figure 4: Isoclines and vector fields in the simplified version of the PLA model. The vertical line at K separates zones above and below the plant's carrying capacity ($x = 1$). Equilibria (intersections) can be stable (black), unstable (white), or unstable focus (@, see text for justification). (A) An always decreasing plant isocline (green) intersects the larva isocline (black) leading to stable coexistence via damped oscillations. (B) Plant isoclines can bulge above K (green+red) and have a hump (blue+green). Intersections at the left of the hump (blue) lead to limit cycles, intersections at the right (green) lead to damped oscillations like in (A). (C) The plant's isocline is like in (B), but the insect's isocline intersects the "fold" (red) of the plant's isocline, resulting in stable equilibria without oscillations. (D) A mushroom-shaped plant's isocline whose decreasing part (green) resembles a logistic prey isocline with enlarged pseudo carrying capacity (K'>1). Isocline intersections can happen once, or twice as depicted, giving rise to Allee effects (this can also happen with plant isoclines like in B,C but never in A).

When the second inequality of (6) widens ($\gamma\sigma\alpha \gg \eta\nu$), the plant's isocline tends to take a mushroom-like shape (or "anvil" or letter "Ω"), as in Figure 4D. Indeed, as γ, σ, α increase and/or η, ν decrease more and more, the decreasing segment of the isocline approximates a decreasing line, while the rest of the isocline is pushed closer and closer to the axes. In other words, when pollination rates (α), benefits (σ), adult lifetimes ($1/\nu$) and larva development rates (γ) increase, plant isoclines would resemble the isocline of a logistic prey, with a "pseudo" carrying capacity (the rightmost extent of the isocline) larger than the intrinsic carrying capacity ($x = 1$). These conditions would promote stable coexistence with large plant equilibrium biomasses.

4 Discussion

We developed a plant–insect model that considers two interaction types, pollination and herbivory. Ours belongs to a class of models (Hernandez, 1998; Holland and DeAngelis, 2010) in which balances between costs and benefits cause continuous variation in interaction strengths, as well as transitions among interaction types (mutualism, predation, competition). In our particular case, interaction types depend on the stage of the insect's life cycle, as inspired by the interaction between *M. sexta* and *D. wrightii* (Bronstein et al., 2009; Alarcon et al., 2008) or between *M. sexta* and *N. attenuata* (Baldwin, 1988). There are many other examples of pollination–herbivory in Lepidopterans, where adult butterflies pollinate the same plants exploited by their larvae (Wäckers et al., 2007; Altermatt and Pearse, 2011). We assign antagonistic and mutualistic roles to larva and adult insect stages respectively, which enable us to study the consequences of ontogenetic changes on the dynamics of plant–insect associations, a topic that is receiving increased attention (Miller and Rudolf, 2011; Rudolf and Lafferty, 2011). Our model could be generalized to other scenarios, in which drastic ontogenetic niche shifts cause the separation of benefits and costs in time and space. But excludes cases like the yucca/yucca moth interaction (Holland et al., 2002), where adult pollinated ovules face larval predation, i.e. benefits themselves are deducted.

Instead of using species biomasses as resource and service proxies (Holland and DeAngelis, 2010), we consider a mechanism (1) that treats resources more explicitly (Encinas-Viso et al., 2014). We use flowers as a direct proxy of resource availability, by assuming a uniform volume of nectar per flower. Nectar consumption by insects is concomitant with service exploitation by the plants (pollination), based on the assumption that flowers contain uniform numbers of ovules. Pollination also leads to flower closure (Primack, 1985), making them limiting resources. Flowers are ephemeral compared with plants and insects, so we consider that they attain a steady-state between production and disappearance. As a result, the dynamics is stated only in terms of plant, larva and adult populations, i.e. the PLA model (3). The feasibility of the results described by our analysis depends on several parameters. The consumption, mortalities and growth rates, and the carrying capacities (e.g. a, b, m, n and r, c in the fourth column of Table 1), have values close to the ranges considered by other models (Holland and DeAngelis, 2010; Johnson and Amarasekare, 2013). Oscillations, for example, require large herbivory rates, but this is usual for *M. sexta* (McFadden, 1968).

4.1 Mutualism–antagonism cycles

The PLA model displays plant–insect coexistence for any combination of (non-trivial) initial conditions where insects can invade when rare ($R_o > 1$). Coexistence is also possible where insects cannot invade when rare ($R_o < 1$), but this requires high initial biomasses of plants and insects (Allee effect). Coexistence can take the form of a stable equilibrium, but it can also take the form of stable oscillations, i.e. limit cycles.

Previous models combining mutualism and antagonism predict oscillations, but they are transient ones (Holland et al., 2002; Wang and Deangelis, 2012), or the limit cycles occur entirely below the plant's carrying capacity (Holland et al., 2013). We have good reasons to conclude that the cycles are herbivory driven and not simply a consequence of the PLA model having many variables and non-linearities. First of all, limit cycles require herbivory rates (β) to be large enough. Second, given limit cycles, an increase in the maturation rate (γ) causes a transition to stable coexistence, and further increase in β is required to induce limit cycles again (Figure 1). This makes sense because by speeding up the transition from larva to adult, the total effect of herbivory on the plants is reduced, hence preventing a crash in plant biomass followed by a crash in the insects. Third, when adult pollinators have alternative food sources ($\phi > 1$), the zone of limit cycles in the space of parameters becomes larger (Figure 3). This also makes sense, because the total effect of herbivory increases by an additional supply of larva (which is not limited by the nectar of the plant considered), leading to a plant biomass crash followed by insect decline.

The graphical analysis provides another indication that oscillations are herbivory driven. On the one hand insect isoclines (or rather larva isoclines) are always positively sloped, and insects only grow when plant biomass is large enough (how large depends on insect's population size, due to intra-specific competition). Plant isoclines,

on the other hand, can display a hump (Figure 4B,C,D), and they grow (decrease) below (above) the hump. These two features of insect and plant isoclines are associated with limit cycles in classical victim–exploiter models (Rosenzweig and MacArthur 1963). If there is no herbivory or another form of antagonism (e.g. competition) but only mutualism, the plant's isocline would be a positively sloped line, and plants would attain large populations in the presence of large insect populations, without cycles. However, mutualism is still essential for limit cycles: if mutualistic benefits are not large enough ($\gamma\sigma\alpha < \eta\nu$), plant isoclines do not have a hump (Figure 4A) and oscillations are predicted to vanish. The effect of mutualism on stability is like the effect of enrichment on the stability in pure victim–exploiter models (Rosenzweig, 1971), by allowing the plants to overcome the limits imposed by their intrinsic carrying capacity (e.g. the pseudo-carrying capacity K' in Figure 4D).

4.2 Classification of outcomes: mutualism or herbivory?

Interactions can be classified according to the net effect of one species on the abundance (biomass, density) of another (but see other schemes Abrams 1987). This classification scheme can be problematic in empirical contexts, because reference baselines such as carrying capacities are usually not known and because stable abundances make little sense under the influence of unpredictable external fluctuations (Hernandez, 2009).

Our PLA model illustrates the classification issue when non-equilibrium dynamics are generated endogenously, i.e. not by external perturbations. Since plants are facultative mutualists and insects are obligatory ones, one can say the outcome is *net mutualism* (+,+) or *net herbivory* (–,+), if the coexistence is stable, and the plant equilibrium ends up respectively above or below the carrying capacity (Hernandez, 1998; Holland and DeAngelis, 2010). If coexistence is under non-equilibrium conditions and plant oscillations are entirely below the carrying capacity (e.g. for large β), the outcome is detrimental for plant and hence there is net herbivory (–,+); oscillations may in fact be considered irrelevant for this conclusion (or may further support the case of herbivory, read below). However, when the plant oscillation maximum is above carrying capacity and the minimum is below, like in Figure 2, could we say that the system alternates periodically between states of net mutualism and net herbivory? Here perhaps a time-based average over the cycle can help up us decide. The situation could be more complicated if plant oscillations lie entirely above the carrying capacity (see an example in Appendix C): one can say that the net outcome is a mutualism due to enlarged plant biomasses, but the oscillations indicates that a victim–exploiter interaction exists. As we can see, deciding upon the net outcome require consideration of both equilibrium and dynamical aspects.

4.3 Factors that could cause dynamical transitions

Environmental factors

The parameters in our analyses can change due to external factors. One of the most important is temperature (Gillooly et al., 2001). It is well known for example, that warming can reduce the number of days needed by larvae to complete their development (Bonhomme, 2000), making γ higher. Keeping everything else equal but γ, for insects that cannot invade when rare (i.e. displaying Allee effects, $R_o < 1$), a cooling of the environment will cause the sudden extinction of the insect and a catastrophic collapse of the mutualism, which cannot be simply reverted by warming. For insects that can invade when rare ($R_o > 1$), by slowing down larva development, cooling would increase the burden of herbivory over the benefits of pollination making the system more prone to oscillations and less stable (even less under strong herbivory, large β). Flowering, pollination, herbivory, growth and mortality rates (e.g. s, a, b, r, m and n in equations 1) are also temperature-dependent, and they can increase or decrease with warming depending on the thermal impacts on insect and plant metabolisms (Vasseur and McCann, 2005). This makes general predictions more difficult. However, we get the general picture that warming or cooling can change the balance between costs and benefits impacting the stability of the plant–insect association.

Dynamical transitions can also be induced by changes in the chemical environment, often as a consequence of human activity. Some pesticides, for example, are hormone retarding agents (Dev, 1986). This means that their release can reduce γ altering the balance of the interaction towards more herbivory and less pollination and finally endangering pollination service (Potts et al., 2010; Kearns et al., 1998). In other cases, the chemical changes are initiated by the plants: in response to herbivory, many plants release predator attractants (Allmann and Baldwin, 2010), which can increase larval mortality μ. If the insect does nothing but harm, this is always an advantage. If the insect is also a very effective pollinator, the abuse of this strategy can cost the plant important pollination services because a dead herbivore today is one less pollinator tomorrow.

Another factor that can increase or decrease larvae maturation rates (γ), is the level of nutrients present in the plant's vegetative tissue (Woods, 1999; Perkins et al., 2004). On the one hand, the use of fertilizers rich in phosphorus

could increase larvae maturation rates (Perkins et al., 2004). On the other hand, under low protein consumption *M. sexta* larvae could decrease maturation rate, although *M. sexta* larvae can compensate this lack of proteins by increasing their herbivory levels (i.e. compensatory consumption) (Woods, 1999). Thus, different external factors related to plant nutrients could indirectly trigger different larvae maturation rates that will potentially modify the interaction dynamics.

Pollinator's diet breadth

An important factor that can affect the balance between mutualism and herbivory is the diet breadth of pollinators. Alternative food sources for the adults could lead to apparent competition (Holt, 1977) mediated by pollination, as predicted for the interaction between *D. wrigthii* (Solanacea) and *M. sexta* (Sphingidae) in the presence of *Agave palmieri* (plant) (Bronstein et al., 2009): visitation of *Agave* by *M. sexta* does not affect the pollination benefits received by *D. wrightii*, but it increases oviposition rates on *D. wrightii*, increasing herbivory. As discussed before, such an increase in herbivory could explain why oscillations are more widespread when adult insects have alternative food sources ($\phi > 0$) in our PLA model.

Although we did not explore this with our model, the diet breadth of the larva could also have important consequences. In the empirical systems that inspired our model, the larva can have alternative hosts (Alarcon et al., 2008), spreading the costs of herbivory over several species. The local extinction of such hosts could increase herbivory on the remaining ones, promoting unstable dynamics. To explore these issues properly, models like ours must be extended to consider larger community modules or networks, taking into account that there is a positive correlation between the diet breadths of larval and adult stages (Altermatt and Pearse, 2011).

From the perspective of the plant, the lack of alternative pollinators could also lead to increased herbivory and loss of stability. The case of the tobacco plant (*N. attenuata*) and *M. sexta* is illustrative. These moths are nocturnal pollinators, and in response to herbivory by their larvae, the plants can change their phenology by opening flowers during the morning instead. Thus, oviposition and subsequent herbivory can be avoided, whereas pollination can still be performed by hummingbirds (Kessler et al., 2010). Although hummingbirds are thought to be less reliable pollinators than moths for several reasons (Irwin, 2010), they are an alternative with negligible costs. Thus, a decline in hummingbird populations will render the herbivore avoidance strategy useless and plants would have no alternative but to be pollinated by insects with herbivorous larvae that promote oscillations.

4.4 Conclusions

Many insect pollinators are herbivores during their larval phases. If pollination and herbivory targets the same plant (e.g. as between tobacco plants and hawkmoths), the overall outcome of the association depends on the balance between costs and benefits for the plant. As predicted by our plant-larva-adult (PLA) model, this balance is affected by changes in insect development: the faster larvae turns into adults the better for the plant, and the more stable the interaction; the slower this development the poorer the outcome for the plant, and the less stable the interaction (oscillations). Under plant–insect oscillations, this balance can be dynamically complex (e.g. periodic alternation between mutualism and antagonism). Since maturation rates play an essential role in long term stability, we predict important qualitative changes in the dynamics due to changes in environmental conditions, such as temperature and chemical compounds (e.g. toxins, hormones, plant nutrients). The stability of these mixed interactions can also be greatly affected by changes in the diet generalism of the pollinators.

Acknowledgements

We thank Rampal Etienne for the discussions that inspired us to write this article. We thank the comments and suggestions from our colleagues of the Centre for Biodiversity Theory and Modelling in Moulis, France, and the Centre for Australian National Biodiversity and Research at CSIRO in Canberra, Australia. TAR was supported by the TULIP Laboratory of Excellence (ANR-10-LABX-41). FEV was supported by the OCE postdoctoral fellowship at CSIRO.

References

Abrams, P. A. (1987). On classifying interactions between populations. *Oecologia 73*(2), 272–281.

Adler, L. S. and J. L. Bronstein (2004). Attracting antagonists: Does floral nectar increase leaf herbivory? *Ecology 85*(6), 1519–1526.

Alarcon, R., G. Davidowitz, and J. L. Bronstein (2008). Nectar usage in a southern Arizona hawkmoth community. *Ecological Entomology 33*(4), 503–509.

Allmann, S. and I. T. Baldwin (2010). Insects betray themselves in nature to predators by rapid isomerization of green leaf volatiles. *Science 329*(5995), 1075–1078.

Altermatt, F. and I. S. Pearse (2011). Similarity and specialization of the larval versus adult diet of european butterflies and moths. *American Naturalist 178*(3), 372–382.

Baldwin, I. T. (1988). The alkaloidal responses of wild tobacco to real and simulated herbivory. *Oecologia 77*(3), 378–381.

Barron-Gafford, G., U. Rascher, J. Bronstein, G. Davidowitz, B. Chaszar, and T. Huxman (2012). Herbivory of wild *Manduca sexta* causes fast down-regulation of photosynthetic efficiency in *Datura wrightii*: an early signaling cascade visualized by chlorophyll fluorescence. *Photosynthesis Research 113*, 249–260.

Bonhomme, R. (2000). Bases and limits to using 'degree.day' units. *European Journal of Agronomy 13*(1), 1–10.

Bronstein, J. L. (1994). Conditional outcomes in mutualistic interactions. *Trends in Ecology and Evolution 9*(6), 214–217.

Bronstein, J. L., T. Huxman, B. Horvath, M. Farabee, and G. Davidowitz (2009). Reproductive biology of Datura wrightii: the benefits of a herbivorous pollinator. *Annals of Botany 103*(9), 1435–1443.

Campbell, C., J. Walgenbach, and G. Kennedy (1991). Effect of Parasitoids on Lepidopterous Pests in Insecticide-Treated and Untreated Tomatoes in Western North Carolina. *Journal of Economic Entomology 84*, 1662–1667.

Case, T. (2000). *An Illustrated Guide to Theoretical Ecology*. Oxford University Press.

Dev, S. (1986). Trends in development of insect growth regulators in plant protection. *Proceedings of the Indian National Science Academy B52*(1), 17–24.

Encinas-Viso, F., T. A. Revilla, and R. S. Etienne (2014). Shifts in pollinator population structure may jeopardize pollination service. *Journal of Theoretical Biology 352*, 24–30.

Fagan, W. F., S. Bewick, S. Cantrell, C. Cosner, I. G. Varassin, and D. W. Inouye (2014). Phenologically explicit models for studying plant-pollinator interactions under climate change. *Theoretical Ecology 7*, 289–297.

Gillooly, J. F., J. H. Brown, G. B. West, V. M. Savage, and E. L. Charnov (2001). Effects of size and temperature on metabolic rate. *Science 293*, 2248–2251.

Hernandez, M. J. (1998). Dynamics of transitions between population interactions: a nonlinear interaction α-function defined. *Proceedings of the Royal Society B: Biological Sciences 265*, 1433–1440.

Hernandez, M. J. (2009). Disentangling nature, strength and stability issues in the characterization of population interactions. *Journal of Theoretical Biology 261*, 107–119.

Holland, J. N. and D. L. DeAngelis (2010). A consumer-resource approach to the density-dependent population dynamics of mutualism. *Ecology 91*, 1286–1295.

Holland, J. N., D. L. DeAngelis, and J. L. Bronstein (2002). Population dynamics and mutualism: functional responses of benefits and costs. *American Naturalist 159*, 231–244.

Holland, J. N., Y. Wang, S. Sun, and D. L. DeAngelis (2013). Consumer-resource dynamics of indirect interactions in a mutualism-parasitism food web module. *Theoretical Ecology 6*(4), 475–493.

Holt, R. D. (1977). Predation, apparent competition, and the structure of prey communities. *Theoretical Population Biology 12*, 197–229.

Irwin, R. E. (2010). Evolutionary ecology: when pollinators are also herbivores. *Current Biology 20*(3), 100–101.

Johnson, C. A. and P. Amarasekare (2013). Competition for benefits can promote the persistence of mutualistic interactions. *Journal of Theoretical Biology 328*, 54–64.

Jones, E., J. Bronstein, and R. Ferriere (2012). The fundamental role of competition in the ecology and evolution of mutualisms. *Annals of the New York Academy of Sciences 1256*, 66–88.

Kearns, C., D. Inouye, and N. Waser (1998). Endangered mutualims: The conservation of plant-pollinator Interactions. *Annual Review of Ecology and Systematics 29*, 83–112.

Kennedy, G. (2003). Tomato, pests, parasitoids, and predators: Tritrophics interactions involving the Genus Lycopersicon. *Annual Review of Entomology 48*, 51–72.

Kessler, D., C. Diezel, and I. T. Baldwin (2010). Changing pollinators as a means of escaping herbivores. *Current Biology 20*(3), 237–242.

McFadden, M. (1968). Observations on feeding and movement of tobacco hornworm larvae. *Journal of Economic Entomology 61*, 352–356.

Miller, T. E. X. and V. H. W. Rudolf (2011). Thinking inside the box: community-level consequences of stage-structured populations. *Trends in Ecology and Evolution 26*(9), 457–466.

Perkins, M., H. Woods, J. Harrison, and J. Elser (2004). Dietary Phosphorus Affects the Growth of Larval *Manduca sexta*. *Archives of Insect Biochemistry and Physiology 53*, 153–168.

Potts, S., J. Biesmeijer, C. Kremen, P. Neumann, O. Schweiger, and W. Kunin (2010). Global pollinator declines: trends, impacts and drivers. *Trends in Ecology and Evolution 25*, 345–353.

Primack, R. B. (1985). Longevity of individual flowers. *Annual Review of Ecology and Systematics 16*, 15–37.

Reinecke, J., J. Buckner, and S. Grugel (1980). Life cycle of laboratory-reared tobacco hornworms, *Manduca sexta*, a study of development and behavior, using time-lapse cinematography. *The Biological Bulletin 158*, 129–140.

Rinaldi, S. and M. Scheffer (2000). Geometric analysis of ecological models with slow and fast processes. *Ecosystems 3*, 507–521.

Rosenzweig, M. L. (1971). The paradox of enrichment. *Science 171*, 385–387.

Rosenzweig, M. L. and R. H. MacArthur (1963). Graphical representation and stability conditions of predator-prey interactions. *American Naturalist 97*, 209–223.

Rudolf, V. H. W. and K. D. Lafferty (2011). Stage structure alters how complexity affects stability of ecological networks. *Ecology letters 14*(1), 75–79.

Schoener, T. W. (1978). Effects of density-restricted food encounter on some single-level competition models. *Theoretical Population Biology 13*(3), 365–381.

Stephens, P. A., W. J. Sutherland, and R. P. Freckleton (1999). What is the Allee effect? *Oikos 87*(1), 185–190.

Vasseur, D. A. and K. S. McCann (2005). Mechanistic approach for modeling temperature-dependent consumer-resource dynamics. *American Naturalist 166*, 184–198.

Wäckers, F. L., J. Romeis, and P. van Rijn (2007). Nectar and pollen feeding by insect herbivores and implications for multitrophic interactions. *Annual Review of Entomology 52*, 301–323.

Wang, Y. and D. L. Deangelis (2012). A mutualism-parasitism system modeling host and parasite with mutualism at low density. *Mathematical Biosciences and Engineering 9*(2), 431–444.

Woods, H. (1999). Patterns and Mechanisms of Growth of Fifth-Instar *Manduca sexta* Caterpillars Following Exposure to Low- or High-Protein Food during Early Instars. *Physiological and Biochemical Zoology 72*, 445–454.

Ziegler, R. (1991). Changes in lipid and carbohydrate metabolism during starvation in adult *Manduca sexta*. *Journal of Comparative Physiology B 161*, 125–131.

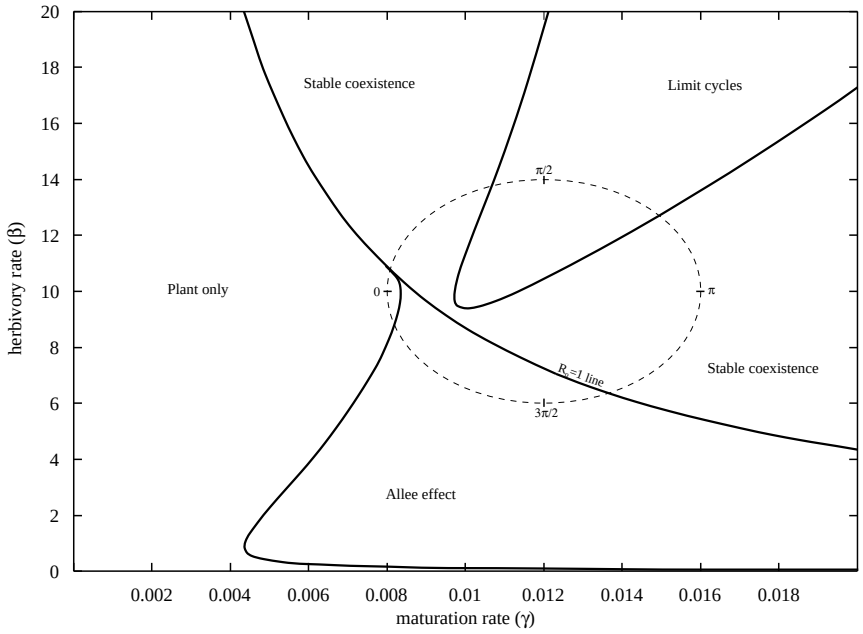

Figure A.1: Outcomes of the PLA model as a function of the larval maturation and herbivory rates for specialist pollinators. The ellipse describes the joint variation of γ and β taking place in the bifurcation diagram in Figure A.2.

Appendices

Appendix A: Bifurcations

Figure 1 in the main text shows all outcomes (plant-only, Allee effect, stable coexistence and limit cycles) occurring together in a rectangle at the bottom left corner of the parameter space β vs γ. We enlarged this rectangle in Figure A.1 in order to show the bifurcations of the PLA model as we traverse the parameter space along an elliptical path as indicated.

From Figure A.2 we can conclude that plant equilibrium biomasses (stable or not) are inversely related with the rate of herbivory (β). A similar response occurs regarding oscillations: as long as β values are large enough to induce oscillations (the part in the figure marked with circles), such oscillations tend to display lower maxima and minima for larger values of β, and higher maxima and minima for smaller values instead.

The response of plant biomasses with respect to the insect maturation rate (γ) is more complex. For example around the middle part of Figure A.2 (between the $\pi/2$ and $3\pi/2$ marks), increasing γ causes (equilibrium) plant biomass increases if herbivory is high, but decreases if herbivory is low. In contrast, increasing γ from very low values causes plant biomass to increase if herbivory is low (between LP and the $3\pi/2$ mark at the right) or decrease when it is high (between BP and the $\pi/2$ mark at the left).

The transitions between stability and limit cycles are typically *super-critical Hopf bifurcations*, in which a stable branch of periodic solutions overlaps a branch of unstable equilibria. The bifurcation diagram (Figure A.2) also displays a *sub-critical Hopf bifurcation*, in which an unstable branch of periodic solutions overlaps stable equilibria. In such cases the long term outcome can be stable coexistence or a limit cycle depending on the initial conditions. Given the parameter values in Table 1, this sub-critical Hopf bifurcation zone was too narrow to be represented in the parameter space (Figure A.1). Appendix C contains a simulation in which a small change in the initial conditions causes the system to approach an equilibrium or a limit cycle.

The $R_o = 1$ line in Figure 1 can be found analytically. To do this, we need to know when the carrying capacity equilibrium switches between stable and unstable, which depends on the eigenvalues of the jacobian matrix of the PLA model (3) evaluated at $(x, y, z) = (1, 0, 0)$:

$$\begin{bmatrix} 1-2x+\frac{\sigma\alpha z}{\eta+z}-\beta y & -\beta x & \frac{\sigma\alpha\eta x}{(\eta+z)^2} \\ \frac{\epsilon\alpha z}{\eta+z}-\gamma\beta y & -\mu-\gamma\beta x & \frac{\epsilon\alpha\eta x}{(\eta+z)^2}+\phi \\ \gamma\beta y & \gamma\beta x & -\nu \end{bmatrix} = \begin{bmatrix} -1 & -\beta & \frac{\sigma\alpha}{\eta} \\ 0 & -\mu-\gamma\beta & \frac{\epsilon\alpha}{\eta}+\phi \\ 0 & \gamma\beta & -\nu \end{bmatrix} \tag{A.1}$$

The eigenvalues of the jacobian are $\lambda_1 = -1$ and:

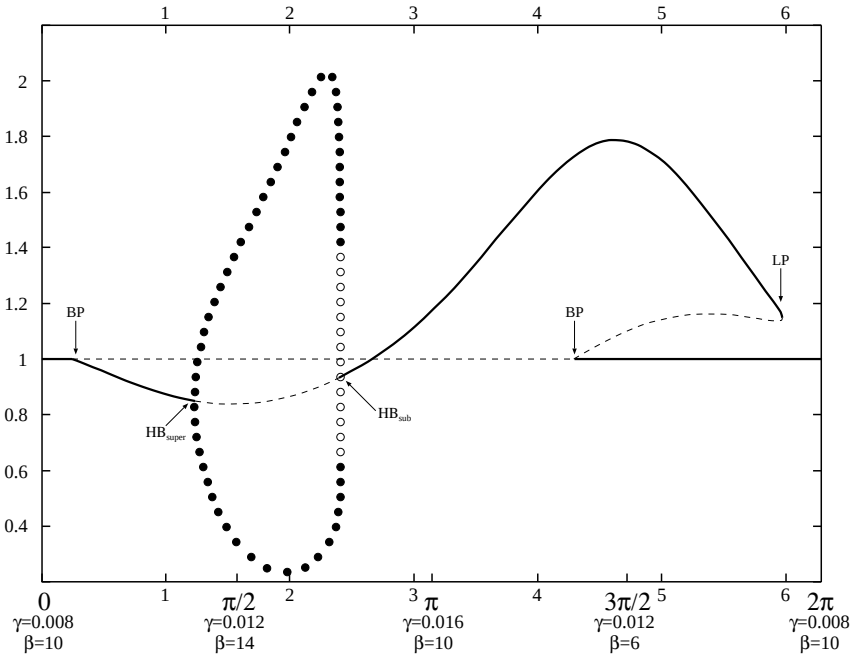

Figure A.2: Bifurcation diagram along the elliptical path drawn in Figure A.1, with reference values of β and γ for each quarter of a rotation. Solid (broken) lines represent stable (unstable) equilibria, black (white) circles represent limit cycle maxima and minima. The $x = 1$ line corresponds to the plant carrying capacity. $\mathrm{HB}_{\mathrm{super}}$: super-critical and $\mathrm{HB}_{\mathrm{sub}}$: sub-critical Hopf bifurcations, BP: branching point (transcritical bifurcation), LP: limit point (fold bifurcation).

$$\lambda_2 = \frac{-(\mu+\nu+\gamma\beta) \pm \sqrt{(\mu+\nu+\gamma\beta)^2 - 4\left[\nu(\mu+\gamma\beta) - \gamma\beta(\phi+\epsilon\alpha/\eta)\right]}}{2}$$

thus $(x, y, z) = (1, 0, 0)$ is unstable if at least one of λ_2 have a positive real part. This can only happen when:

$$\frac{(\epsilon\alpha+\phi\eta)\gamma\beta}{\eta\nu(\mu+\gamma\beta)} > 1 \tag{A.2}$$

by which automatically both λ_2 are real (one is negative and the other is positive). The right-hand side of (A.2) is R_o in the main text. Making $R_o = 1$ and writing β as a function of γ, we obtain a decreasing hyperbolic line with asymptotes $\beta = 0$ and $\gamma = 0$ as shown in Figures 1 and 3. This is yet another reason, a pure technical one this time, that explains why we choose to present our results in the form of a β vs γ parameter space.

Since the eigenvector of λ_1 is a multiple of $(1, 0, 0)$, the eigenvectors of λ_2 are orthogonal to $(1, 0, 0)$, i.e. $v = (0, v_y, v_z), w = (0, w_y, w_z)$. This, and the fact that both λ_2 are real if the inequality above holds, means that only perturbations in y and/or z, i.e. an insect invasion, would make $(x, y, z) = (1, 0, 0)$ unstable.

Appendix B: Isocline properties

Let us assume that the adult phase is very short lived compared with the larval phase and with the dynamics of the plant. In the same way as we did in the case of the flowers, assume that the adults reach a steady-state $dz/dt \approx 0$ with respect to the other variables, and that the adult biomass can be approximated by $z \approx \gamma\beta xy/\nu$. Substituting this in the ODE system (3), we obtain the two-dimensional system:

$$\begin{aligned}
\dot{x} &= x(1-x) + \sigma\frac{\alpha\gamma\beta x^2 y}{\eta\nu+\gamma\beta xy} - \beta xy \\
\dot{y} &= \epsilon\frac{\alpha\gamma\beta x^2 y}{\eta\nu+\gamma\beta xy} + \frac{\phi\gamma\beta xy}{\nu} - \gamma\beta xy - \mu y
\end{aligned} \tag{B.1}$$

This system has two trivial isoclines, $x = 0$ for the plant and $y = 0$ for the insect. The following results only concern the non-trivial isoclines for plants and insects.

Plant isocline

Making $\dot{x} = 0$ in (B.1), the (non-trivial) isocline of the plant can be written as a polynomial in x and y:

$$x^2y + \beta xy^2 - (1 + \sigma\alpha)xy + \frac{\eta\nu}{\gamma\beta}x + \frac{\eta\nu}{\gamma}y - \frac{\eta\nu}{\gamma\beta} = 0 \tag{B.2}$$

To characterize the shape of (B.2) we start by finding asymptotes. To do this we can rewrite (B.2) as a function of x:

$$y(x) = \frac{1}{2\beta}\left\{\frac{-\left(\frac{\eta\nu}{\gamma} - (1+\sigma\alpha)x + x^2\right) \pm \sqrt{\left(\frac{\eta\nu}{\gamma} - (1+\sigma\alpha)x + x^2\right)^2 + 4\frac{\eta\nu}{\gamma}x(1-x)}}{x}\right\} \tag{B.3}$$

We divide the numerator and the denominator of (B.3) by x:

$$\begin{aligned} y(x) &= \frac{1}{2\beta}\left\{-\frac{\eta\nu}{\gamma x} + (1+\sigma\alpha) - x \pm \sqrt{\frac{1}{x^2}\left(\frac{\eta\nu}{\gamma} - (1+\sigma\alpha)x + x^2\right)^2 + \frac{1}{x^2}4\frac{\eta\nu}{\gamma}x(1-x)}\right\} \\ &= \frac{1}{2\beta}\left\{-\frac{\eta\nu}{\gamma x} + (1+\sigma\alpha) - x \pm \sqrt{\left(\frac{\eta\nu}{\gamma x} - (1+\sigma\alpha) + x\right)^2 + 4\frac{\eta\nu}{\gamma}\left(\frac{1}{x} - 1\right)}\right\} \end{aligned}$$

and we take the limit when x goes to plus or minus infinity:

$$\begin{aligned} \lim_{x\to\pm\infty} y(x) &= \frac{1}{2\beta}\lim_{x\to\pm\infty}\left\{0 + (1+\sigma\alpha) - x \pm \sqrt{(0 - (1+\sigma\alpha) + x)^2 + 4\frac{\eta\nu}{\gamma}(0-1)}\right\} \\ &= \frac{1}{2\beta}\lim_{x\to\pm\infty}\left\{-(x - 1 - \sigma\alpha) \pm \sqrt{(x-1-\sigma\alpha)^2 - 4\frac{\eta\nu}{\gamma}}\right\} \end{aligned}$$

Note that $|x - 1 - \sigma\alpha| > \sqrt{(x-1-\sigma\alpha)^2 - 4\frac{\eta\nu}{\gamma}}$. Thus, the square root above can be approximated by $\delta(x)(x - 1 - \sigma\alpha)$, where δ is a number between 0 and 1, and $\delta(x) \to 1$ as $x \to \pm\infty$. We can continue as follows:

$$\begin{aligned} \lim_{x\to\pm\infty} y(x) &= \frac{1}{2\beta}\lim_{x\to\pm\infty}\{-(x - 1 - \sigma\alpha) \pm \delta(x)(x - 1 - \sigma\alpha)\} \\ &= \frac{x - 1 - \sigma\alpha}{\beta}\lim_{x\to\pm\infty}\frac{\{-1 \pm \delta(x)\}}{2} \end{aligned} \tag{B.4}$$

When $x \to \pm\infty$ and $\delta \to 1$, the '+' branch, $y(x)$ approaches the horizontal asymptote $y = 0$. For this '+' branch we also have that $-1 < \{-1 + \delta(x)\} < 0$ in (B.4), which means that y is negative when $x \to +\infty$, and positive when $x \to -\infty$. In other words, the horizontal asymptote is approached from below when $x \to +\infty$ and from above when $x \to -\infty$.

When $x \to \pm\infty$ and $\delta \to 1$, the '–' branch, $y(x)$ approaches the slanted asymptote:

$$y = \frac{1 + \sigma\alpha - x}{\beta} \tag{B.5}$$

which decreases with x. For this '–' branch we also have that $-1 < \{-1 - \delta(x)\}/2 < -1/2$ in (B.4), which means that when $x \to +\infty$, $y < 0$ and $|y| < |(x - 1 - \sigma\alpha)/\beta|$. In other words, y lies between 0 and the slanted asymptote when $x \to +\infty$.

If we write (B.2) as a function of y rather than as a function of x, we will find a vertical asymptote $x = 0$, and the slanted asymptote (B.5) again. Because (B.2) is symmetric regarding the signs of its terms, the properties of the vertical asymptote must consistent with those of the horizontal: $y(x)$ goes towards $+\infty$ when $x = 0$ is approached from the left, and towards $-\infty$ when $x = 0$ is approached from the right. Also because of symmetry x must lie between 0 and the slanted asymptote when $y \to +\infty$.

The following statements tells us the location of special points of (B.2) as well regions in which (B.2) cannot be satisfied.

Lemma 1: the plant isocline contains the following (x, y) points:

$$\begin{aligned} \mathrm{K} &= (1, 0) \\ \mathrm{O} &= (0, \beta^{-1}) \\ \mathrm{P} &= (\sigma\alpha - \eta\nu\gamma^{-1}, \beta^{-1}) \\ \mathrm{Q} &= (1, (\sigma\alpha - \eta\nu\gamma^{-1})\beta^{-1}) \end{aligned} \tag{B.6}$$

Proof: evaluate (B.2) at $x = 1$ to get a quadratic equation in y with roots $y = 0$ and $y = (\sigma\alpha - \eta\nu/\gamma)/\beta$, this gives points K and Q respectively. Evaluate (B.2) at $y = \beta^{-1}$ to get a quadratic equation in x with roots $x = 0$ and $x = \sigma\alpha - \eta\nu/\gamma$, this gives points O and P respectively. Points K (the plant's carrying capacity), and O are always biologically feasible (both have non-negative coordinates).

Corollary 1: Simple observation of (B.6) tells us that points P and Q are simultaneously biologically feasible if $\gamma\sigma\alpha > \eta\nu$. Conversely, both are unfeasible if $\gamma\sigma\alpha < \eta\nu$.

Lemma 2: Points P and Q lie below the slanted asymptote (B.5).

Proof: substitute $y = \beta^{-1}$ in (B.5) to obtain point $(\sigma\alpha, \beta^{-1})$, and substitute $x = 1$ in (B.5) to obtain point $(1, \sigma\alpha/\beta)$. Simple inspection shows that point $(\sigma\alpha, \beta^{-1})$ is always to the right of point P, and point $(1, \sigma\alpha/\beta)$ is always above point Q.

Lemma 3: the plant isocline crosses the x- and y-axis only at points K and O respectively, and nowhere else.

Proof: substituting $y = 0$ in (B.2) gives only one root $x = 1$ (i.e. point K). Substituting $x = 0$ in (B.2) gives only one root $y = \beta^{-1}$ (i.e. point O).

Lemma 4: the plant isocline is not satisfied in the $(-, -)$ quadrant.

Proof: let $a, b \geq 0$ and substitute $x = -a$ and $y = -b$ in (B.2). This leads to:

$$-\left[a^2 b + \beta a b^2 + (1 + \sigma\alpha)ab + \frac{\eta\nu}{\gamma\beta}a + \frac{\eta\nu}{\gamma}b + \frac{\eta\nu}{\gamma\beta}\right] = 0 \tag{B.7}$$

since all parameter values are positive, the statement above is false, thus (B.2) is not satisfied in the $(-, -)$ quadrant.

Using this information about the asymptotes ($x = 0, y = 0$ and eq. B.5), and Lemmas 1, 2, 3 and 4 we can conclude that the plant's isocline must have one of the two forms depicted in figure B.1. Corollary 1 explains the form taken in figure B.1A, when $\gamma\sigma\alpha < \eta\nu$, and the form in figure B.1B, when $\gamma\sigma\alpha > \eta\nu$. These are the two main cases referenced in the main text by (6), where only the positive quadrant is considered. For points between the O–K segment and the axes $\dot{x} > 0$, otherwise $\dot{x} < 0$.

Figure B.2 shows how the positive part of the plant isocline changes as we vary some of the bifurcation parameters. Increasing γ or decreasing η or ν, causes the isocline to be "compressed" against the asymptote (B.5) and it adopts the shape of a mushroom, the letter Ω or an anvil. Increasing β causes points P and Q to decrease along the vertically axis. It is more difficult to follow the effect of the rest of the parameters, for example increasing σ and α cause P and Q to move right and upwards respectively, but they also move the asymptote (B.5) right and upwards, so we cannot tell if this will cause the isocline to adopt a mushroom shape.

Larva isocline

Making $\dot{y} = 0$ in (B.1) the larva isocline is:

$$y(x) = \frac{p(x)}{q(x)} \tag{B.8}$$

where the numerator and denominator:

$$p(x) = \epsilon\alpha\gamma\beta x^2 - \eta\nu\gamma\beta(1 - \phi/\nu)x - \eta\mu\nu \tag{B.9}$$

$$q(x) = \gamma\beta\left[\gamma\beta(1 - \phi/\nu)x + \mu\right]x \tag{B.10}$$

are second order polynomials, i.e. parabolas. By assuming instead $\dot{y} > 0$ one obtains (B.8) but with a "$>$" sign, which means that insect biomass grows for points lying below the isocline and conversely decline for points above the isocline.

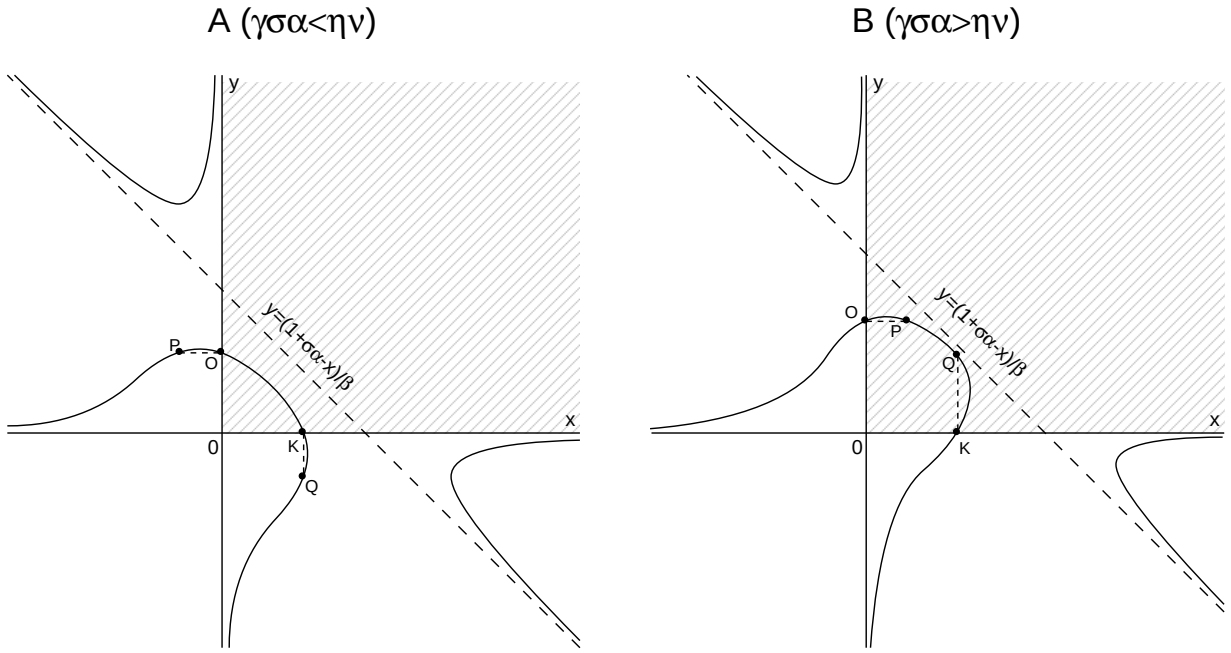

Figure B.1: The two main configurations of the plant isocline. We only consider the O–K segment in the positive octant (hatched square). In A the isocline lies below the plant's carrying capacity (i.e. left of K), in B parts of the isocline lie above (i.e. right of K).

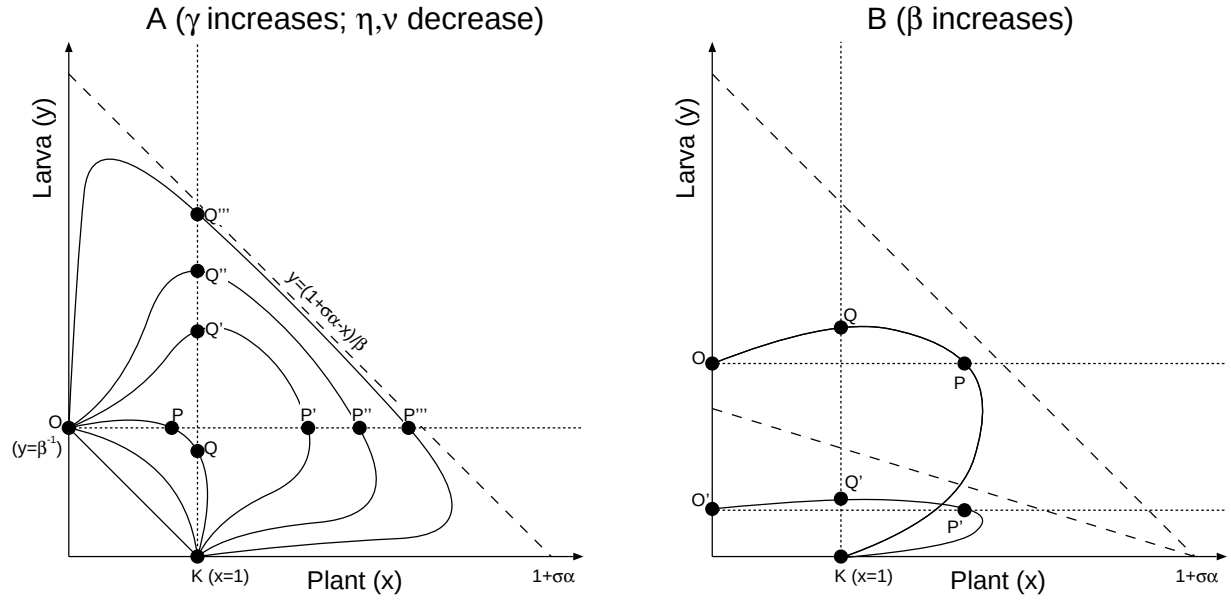

Figure B.2: Changes in the shape of the plant's isocline. (A) As γ increases and η, ν decrease, points P and Q move closer to the diagonal asymptote (broken line), and the isocline eventually adopts the form of a mushroom. (B) As β increases, O, P, Q and the diagonal asymptote move towards the plant axis and the isocline is compressed vertically.

For function $p(x)$: $p(0) = -\eta\mu\nu < 0$ and $\lim_{x\to\pm\infty} p(x) = +\infty$. This means that $p(x)$ has one negative root and one positive root; and also that $p(x) < 0$ between the negative and positive roots, and $p(x) > 0$ otherwise. Since $p(x)$ is the denominator of (B.8), the larva isocline has the same roots as $p(x)$ in the x-axis. The positive root of (B.9) and (B.8) is:

$$x_0 = \frac{\eta\nu}{2\epsilon\alpha}\left(1 - \frac{\phi}{\nu}\right) + \sqrt{\left[\frac{\eta\nu}{2\epsilon\alpha}\left(1 - \frac{\phi}{\nu}\right)\right]^2 + \frac{\eta\mu\nu}{\epsilon\alpha\gamma\beta}} \tag{B.11}$$

For function $q(x)$: it has one root at $x = 0$, a second one at:

$$x_v = -\frac{\mu}{\gamma\beta(1 - \phi/\nu)} \tag{B.12}$$

and $\lim_{x\to\pm\infty} p(x) = -\infty$. This means that $q(x) > 0$ between 0 and x_v, and $q(x) < 0$ otherwise. Both roots make the denominator of (B.8) equal to zero, which means that the larva isocline has two vertical asymptotes, $x = 0$ and x_v.

And finally, the larva isocline has one horizontal asymptote:

$$y_h = \lim_{x\to\pm\infty} \frac{p(x)}{q(x)} = \frac{\epsilon\alpha}{\gamma\beta(1 - \phi/\nu)} \tag{B.13}$$

Notice that the signs of x_v and y_h depend on ϕ/ν:

$$\begin{cases} \phi < \nu: & x_v < 0, y_h > 0 \\ \phi > \nu: & x_v > 0, y_h < 0 \end{cases} \tag{B.14}$$

This information about the parabolas $(p(x), q(x))$, and the signs of the asymptotes (x_v, y_h), is enough to sketch the possible shapes of the larva isocline: the isocline crosses the x-axis at the roots of $p(x)$; its jumps to infinity at the roots of $q(x)$; and is positive (negative) whenever $p(x)$ and $q(x)$ have the same (different) signs. According to (B.14) we have two main cases:

1. If $\phi < \nu$ the vertical asymptote x_v is negative and the horizontal asymptote y_h is positive. As we can see, there are two alternatives, depicted by Figure B.3A and B. Both are indistinguishable in the positive octant, which is the only part that matters: they both start at the x_0 in the plant axis and grow up to a plateau y_h.

2. If $\phi > \nu$ the vertical asymptote x_v is positive and the horizontal asymptote y_h is negative. In this configuration we also have two alternatives, as depicted in Figures B.3C or D. However, we can quickly dismiss alternative D: the insect is meant to grow for points that are below the larva isocline, but since the isocline is decreasing, this automatically means to grow when plant abundance is low rather than high. This is nonsensical because the plant always has a positive effect on insects.

Figure B.4 shows how the positive part of the larva isocline responds to some parameter changes. From the equations that define the isocline's root (B.11) and asymptotes (B.12,B.13) we can conclude that increasing γ, β tends to move the isocline closer to the larva axis.

Appendix C: Additional simulations

Figure C.1 displays limit cycles in the PLA model with plant biomasses entirely above the carrying capacity. The parameters are as in Table 1 of the main text, but with $\gamma = 0.00973, \beta = 0.01$. Figure C.2 shows an example where oscillations can damped out or evolve towards a limit cycle depending on the initial conditions. Parameters as in Table 1 of the main text, but with $\gamma = 0.06, \beta = 20, \nu = 5$. The attraction basins for both outcomes are separated by an unstable orbit, like the one show in the bifurcation plot in Appendix A.

Figure C.3 displays the dynamics of plants, flowers, larva and adult insects under the interaction mechanism (1) from which the PLA model is derived in the main text. This simulation uses parameter values from the last column of Table 1 with $\gamma = 0.01, b = 0.005$. This figure is comparable to Figure 2 in the main text: the 200 time in units there, become $t = \tau/r = 200/0.05 = 4000$ time units here, and the plant's carrying capacity there ($x = 1$), becomes $c^{-1} = 0.01^{-1} = 100$ here.

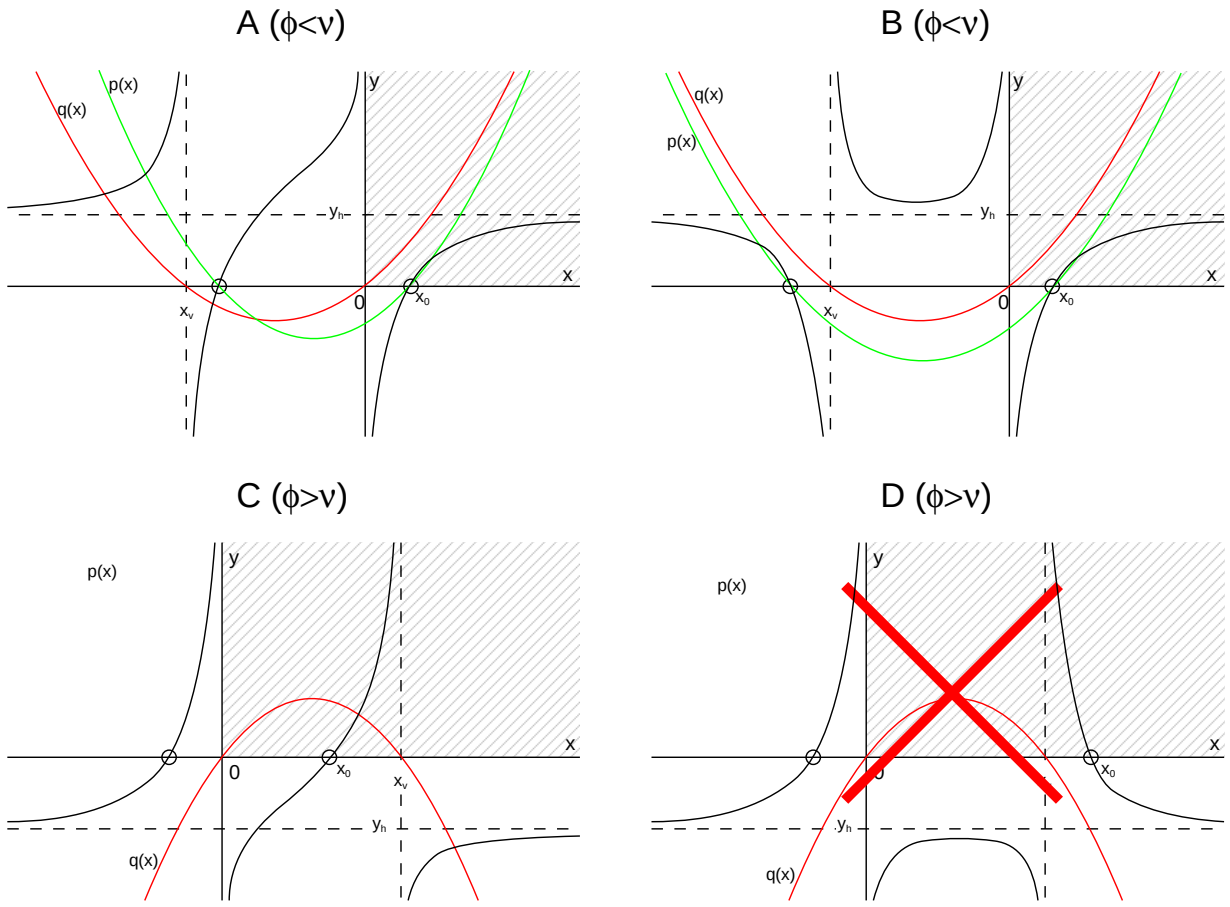

Figure B.3: Possible configurations of the larva isocline, pictured as a three segment black line. For A and B $\phi < \nu$. For C and D $\phi > \nu$. Only parts in the positive octant (hatched square) are considered. The green parabola $p(x)$ is the numerator of the isocline and the circles indicate its roots, where x_0: positive root. The red parabola $q(x)$ is the denominator of the isocline, which has two roots $x = 0$ and $x = x_v$, both of which are also the vertical asymptotes of the isocline. The isocline also has an horizontal asymptote y_h. The alternative in part D can be dismissed because it implies a detrimental effect of plants on insects.

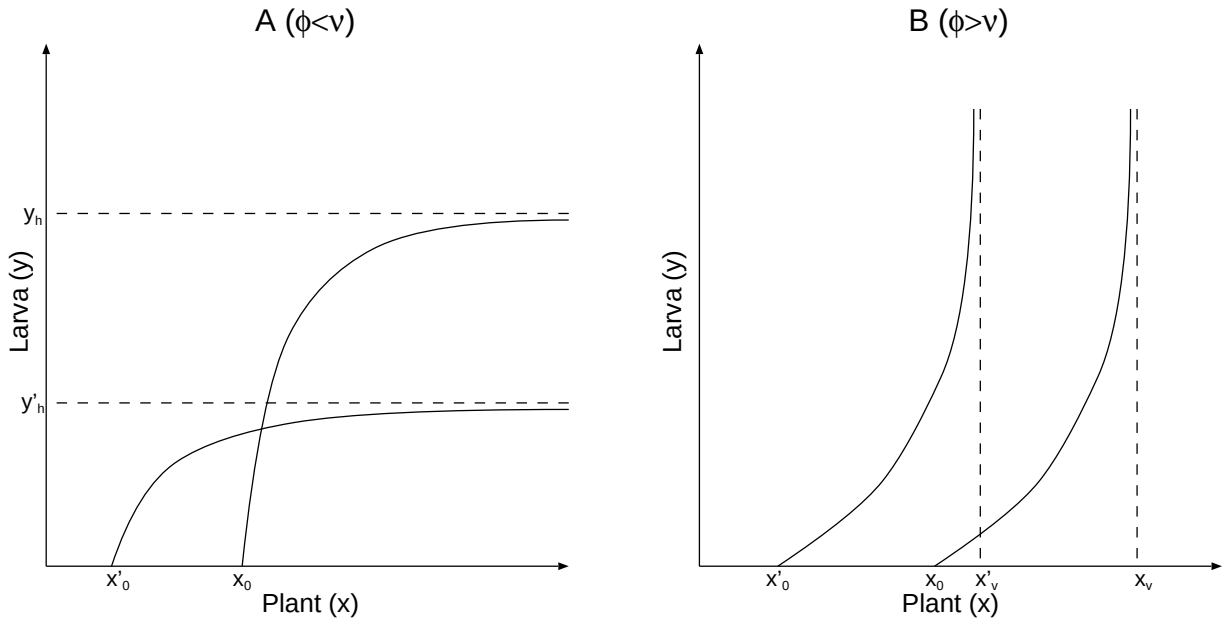

Figure B.4: (A) For $\phi < \nu$ the larva isocline moves closer to the larva axis and becomes more shallow as γ and β increase. For $\phi > \nu$ the larva isocline becomes closer to the larva axis.

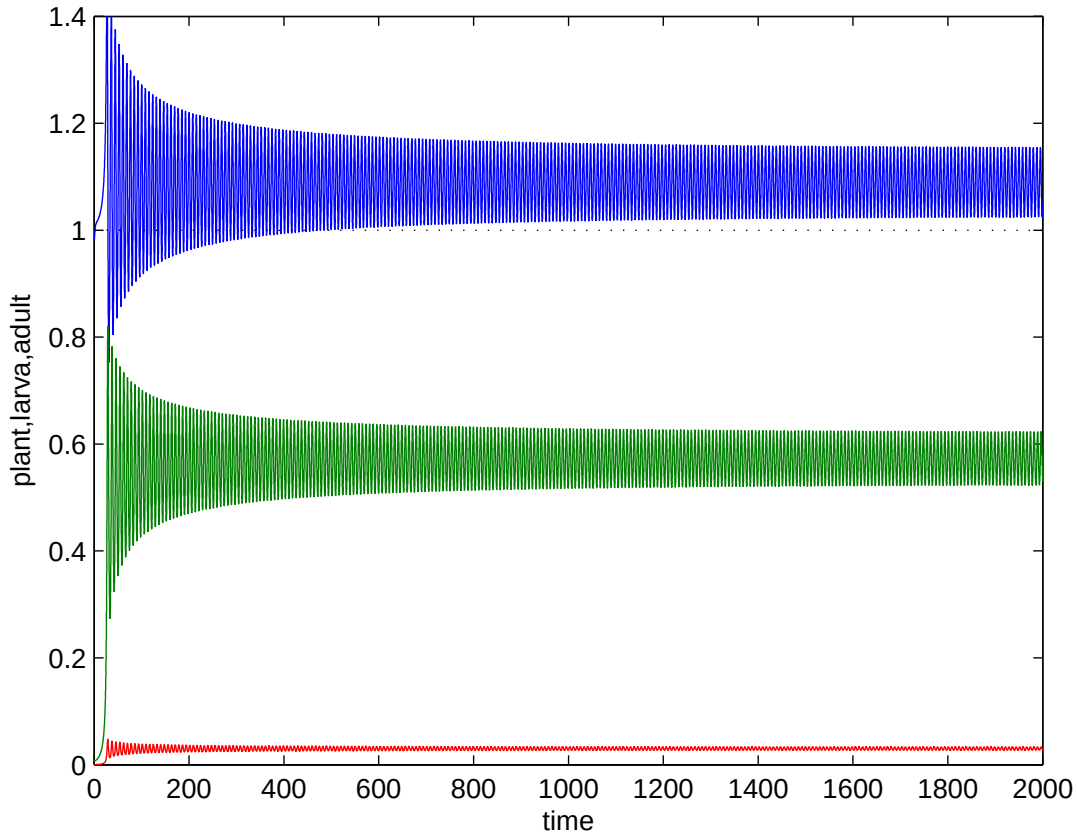

Figure C.1: Limit cycles in the PLA model, with plants above the carrying capacity (dotted line). Blue:plant, green:larva, red:adult.

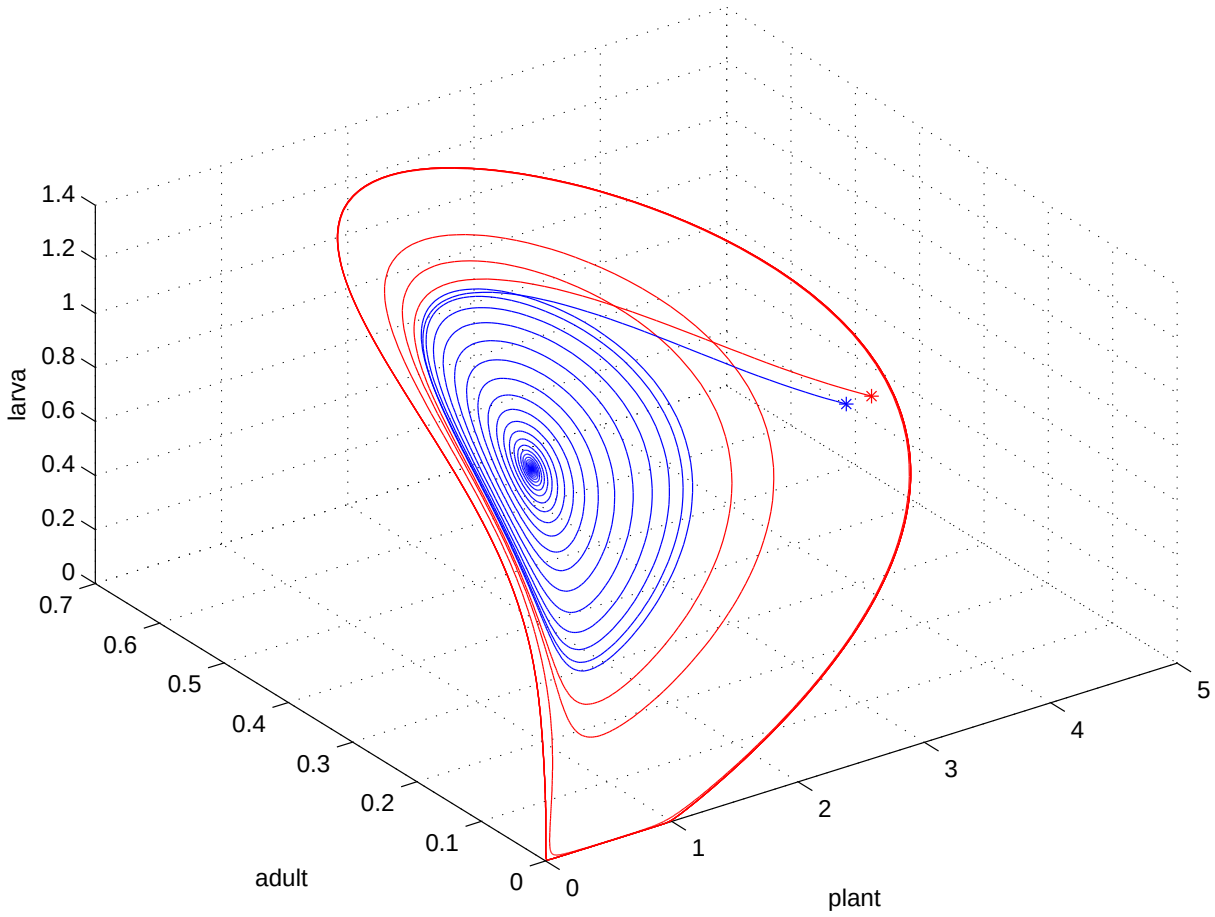

Figure C.2: Oscillations in the PLA model started with different initial conditions (*). The oscillations can dampen out (blue) or converge to a limit cycle (red).

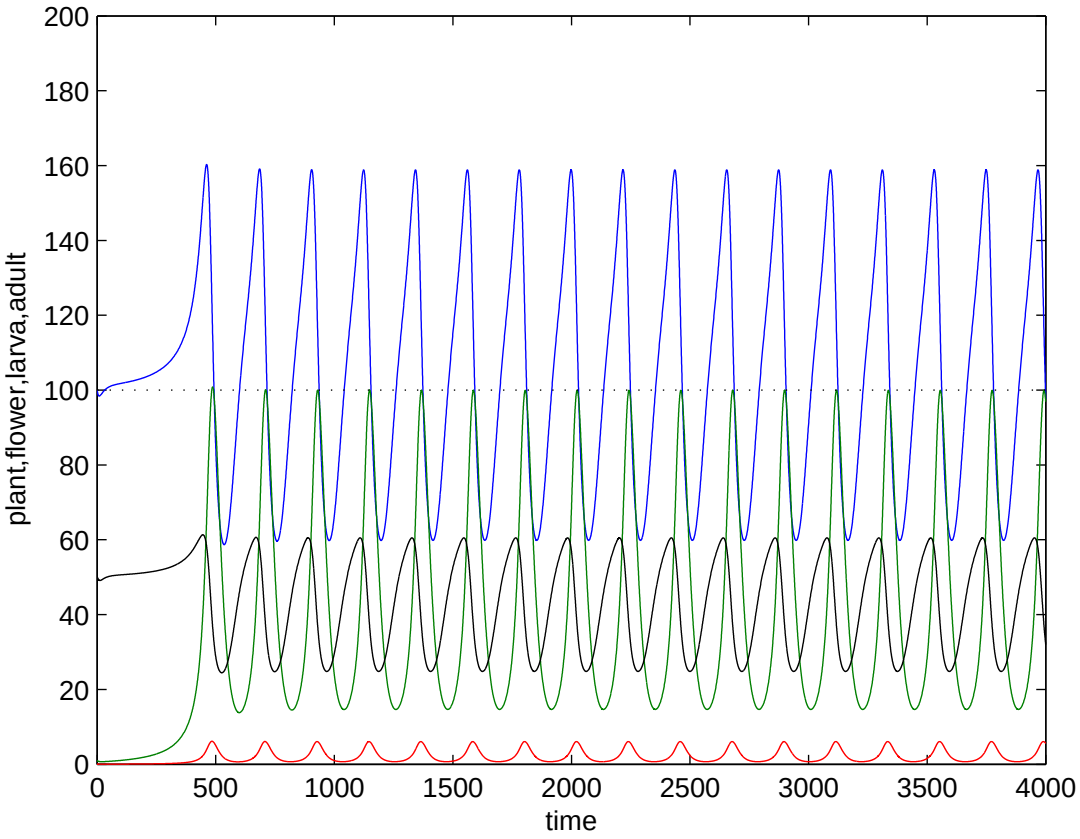

Figure C.3: Interaction dynamics of plants, larva and adults, with the flowers explicitly considered. Blue:plant, green:larva, red:adult, black:flowers. The dotted line indicates the plant's carryng capacity.

608

610